Temperature and doping dependence of non-Gaussian 1/*f* noise and noise statistics in hydrogenated amorphous silicon

G. M. Khera* and J. Kakalios
School of Physics and Astronomy, University of Minnesota, Minneapolis, Minnesota 55455
(Received 11 October 1996; revised manuscript received 19 March 1997)

Coplanar conductance fluctuations in hydrogenated amorphous silicon have been measured as a function of doping type and temperature and are found to have an inverse frequency ($1/f$) spectral density. The $1/f$ noise statistics are non-Gaussian as reflected by (i) strong correlations of the noise power across frequency space and (ii) a power-law second spectrum. The $1/f$ noise and $1/f$ noise statistics exhibit weak doping and temperature dependences. The results are discussed in terms of a model for electronic conduction involving inhomogeneous current filaments whose conductance is modulated by hydrogen diffusion. The growth of the frequency correlation coefficients with averaging time, the variation of the magnitudes of the correlation coefficients with the magnitudes of the second spectrum, and the scaling properties of the second spectra are consistent with the presence of hierarchical kinetics. [S0163-1829(97)05728-7]

I. INTRODUCTION

In *n*-type and undoped hydrogenated amorphous silicon (*a*-Si:H), statistical tests of the coplanar conductance fluctuations (fluctuations that have a $1/f$ spectral density for frequency f) have shown that the $1/f$ noise is strongly non-Gaussian.[1–3] There are large correlations of the noise power at differing frequencies, and the second spectrum, which characterizes the time-dependent fluctuations in the noise power, has an approximately $1/f$ frequency dependence; that is, the $1/f$ noise has $1/f$ noise.[1–6] These results indicate that the $1/f$ noise is not simply due to an ensemble set of appropriately distributed independent Lorentzian fluctuators,[4,7] but instead may involve interactions such as serial kinetics that can be described on a hierarchical space.[4,8–11] Further, *a*-Si:H displays intermittent random telegraph switching noise (RTSN) in large-volume samples[12–14] and the $1/f$ noise has a nonlinear dc dependence.[15] In addition to this nontrivial noise dynamics, *a*-Si:H displays glassy behavior reflected in changes in the defect structure and conductivity at an equilibration temperature T_E, which has been likened to a glass-transition temperature.[16,17] Below T_E the defect structure slowly relaxes with a stretched exponential time dependence, while above T_E the defect structure is in thermal equilibrium and is independent of thermal history. Hydrogen motion can change the bonding configurations of the Si and dopant atoms, enabling metastable changes in the defect structure. Studies of the stretched exponential relaxation are found to be in quantitative agreement with the macroscopic dispersive hydrogen diffusion coefficient, indicating that hydrogen diffusion is responsible for the glassy behavior. Recently, dynamical percolation simulations[13] in conjunction with NMR measurements[18,19] have demonstrated that local hydrogen diffusion may be responsible for RTSN (Ref. 14) in *a*-Si:H. However, while it is plausible that hydrogen motion also underlies the time dependence of the $1/f$ noise power fluctuations, direct evidence linking the glasslike kinetics and the $1/f$ noise has been lacking.

In this experimental paper, we explore the roles of the dopant and hydrogen diffusion on the $1/f$ noise and the statistical properties of the $1/f$ noise in undoped, *n*-type, and *p*-type *a*-Si:H as a function of temperature. In Sec. II we give details of the *a*-Si:H samples and the experimental setup. The methodology for the statistical analysis and the results are given in Sec. III. A detailed discussion of the results is presented in Sec. IV, which are summarized in Sec. V.

II. SAMPLES AND EXPERIMENTAL SETUP

All of the *a*-Si:H films studied here were deposited in a plasma-enhanced chemical vapor deposition reactor using silane (SiH_4) gas under standard deposition parameters known for producing high-electronic-quality films. The undoped *a*-Si:H films were deposited at the University of Minnesota; the substrate temperature was 250 °C and the incident rf power was 3 W over an electrode area of ~ 50 cm^2. Both the *n*-type and *p*-type films were synthesized under similar deposition conditions at Xerox PARC. The *n*-type film was doped using phosphine (PH_3) with a gas-phase doping level of 10^{-3} $[PH_3]/[SiH_4]$. Previous measurements on this film have been reported elsewhere.[2] The *p*-type film was doped with diborane (B_2H_6) with the gas-phase doping level also set at 10^{-3} $[B_2H_6]/[SiH_4]$. Using electron-beam evaporation, chromium electrodes were deposited on the *p*-type film. These 1-μm-thick films were patterned using photolithography and reactive ion etching (undoped and *p*-type *a*-Si:H) or ion milling (*n*-type *a*-Si:H) yielding an area 800 μm long by 200 μm wide; the effective sample volume is 1.6×10^{-7} cm^3. Coplanar conductance fluctuation measurements are performed using the two-probe technique with an electrode separation of 800 μm. Electrical leads are attached to the *a*-Si:H using silver paint, which yields linear current-voltage characteristics. The sample resides in the measurement chamber in the dark in an oil-free vacuum and sits on a copper block containing resistive heaters and a cooling line for temperature control. The voltage is applied using a

Hewlett-Packard E3612A power supply and the current is amplified by an Ithaco 564 current preamplifier. The amplified signal is then fast Fourier transformed to calculate the noise power spectral density using a Stanford Research System spectrum analyzer (SR760). The applied voltage is adjusted at each temperature for each a-Si:H film in order to maintain the current at set values between 0.2 and 2.0 μA. In all cases the current is sufficiently large to yield spectral densities at least two orders of magnitude above the background noise level. To ensure that the noise is not due to electrical contact effects, four-probe measurements have been performed on the n-type film. Further, other electrical contact schemes have been employed including mesa structures consisting of a Cr layer on top of an $n+$ (highly doped) layer[2] and conducting epoxy contacts[20] that exhibit similar non-Gaussian $1/f$ noise properties.

III. STATISTICAL METHODS AND RESULTS

Fluctuations of some quantity about its dc value are typically characterized by statistical quantities such as the average, variance, and two-point correlation function. For a Gaussian noise source all statistical information is contained in these quantities. A complete characterization of non-Gaussian noise must involve higher-order correlation functions.[21,22] In Sec. III A we present the power spectral density (PSD) of the noise, which is essentially the Fourier transform of the two-point autocorrelation function and gives the variance of the signal at specific frequencies. In Sec. III B we present a correlation coefficient analysis of the noise in a-Si:H that reveals its non-Gaussian nature. In Sec. III C we describe the non-Gaussian noise in a-Si:H in terms of a four-point correlation function termed the second spectrum.

A. Noise power spectral density

Representative examples of the noise power spectral density (termed the first spectra or S_1 to distinguish it from the second spectra S_2) for the undoped, n-type, and p-type a-Si:H films at 435 K are shown in Fig. 1, over the frequency range from approximately 4 Hz to over 1.5 kHz. This temperature was chosen so that comparable currents could be compared for the high-resistance undoped film and the less-resistive doped samples. Each curve is constructed by rms averaging 1024 rapidly acquired spectra. The dc through the undoped and p-type films was 0.3 μA, while the current was 2.0 μA for the n-type film. Since the noise power in the n-type film at this temperature depends on the square of the dc, the n-type data of Fig. 1 have been scaled from 2.0 to 0.3 μA in order to facilitate comparison with the undoped and p-type films. The issue of the current dependence of the noise has been described elsewhere[2,15,23] and is not a focus of this work.

As is evident in Fig. 1, the noise power is largest for the n-type film and smallest for the undoped film, while the sample geometry, temperature, and current are identical for all three samples. The resistance of the samples are not identical, however. At 435 K, the n-type, p-type, and undoped samples had resistances of approximately 2, 25, and 500 MΩ, respectively. Assuming that the noise power scales with the square of the current, then it is expected that there is an

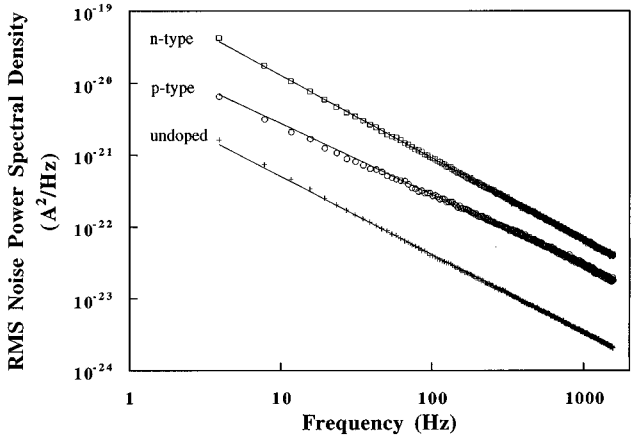

FIG. 1. Representative noise power spectra for the a-Si:H at 435 K and a dc current of 0.3 μA. Each spectrum is calculated by rms averaging 1024 individual spectra. The spectral slopes are $\gamma_1 = 1.14$, 0.99, and 1.09 for the n-type, p-type, and undoped a-Si:H, respectively. The data for the n-type a-Si:H sample were acquired at 2.0 μA and were rescaled to 0.3 μA, as explained in the text.

equivalency between the current noise power S_I and the resistance noise power S_R:[24,25] $S_I/I^2 = S_R/R^2$. Using this relationship, we calculate the intrinsic fractional resistance fluctuations $\delta R/R$ to be $\sim 5\times 10^{-5}$ at 100 Hz and independent of doping type. It is important to note (as described below) that the noise in a-Si:H varies strongly with time. The averaged spectra in Fig. 1 may typically vary by as much as a factor of 5 over a period of many hours while under unchanging external conditions or after high-temperature annealing. Nevertheless, the general trend indicated in Fig. 1 holds.

The noise in the n-type and undoped films displays, at best, a weak temperature dependence. For the n-type and undoped film at a given current, the noise power increased by roughly one order of magnitude over the temperature range from 310 to 435 K and from 435 to 485 K, respectively. Similar behavior was found for thermoelectric $1/f$ noise of various n-type a-Si:H samples.[26,27] The $1/f$ noise magnitude of the p-type sample was measured at 330, 370, 410, and 435 K. The noise power increased by nearly three orders of magnitude from 330 to 410 K (when measured at the same current) and then leveled off at higher temperatures.

B. Correlation coefficients

The power spectral density analysis presented above yields the time-averaged noise spectrum by averaging the individual spectra. This method eliminates any time dependence of the noise. Alternatively, one may consider the frequency and time dependence of the noise via a short-time Fourier transform procedure. In this case the noise characterization involves statistical analysis of the variations of the individual 10^3-10^4 noise power spectra.[4,5,7] In most electronic spectrum analyzers each noise power spectrum consists of 400 frequency bins or fast Fourier transform (FFT) points. In order to enhance the sensitivity to non-Gaussian effects and for computational ease, each individual FFT spectrum is reduced to seven points by summing the fre-

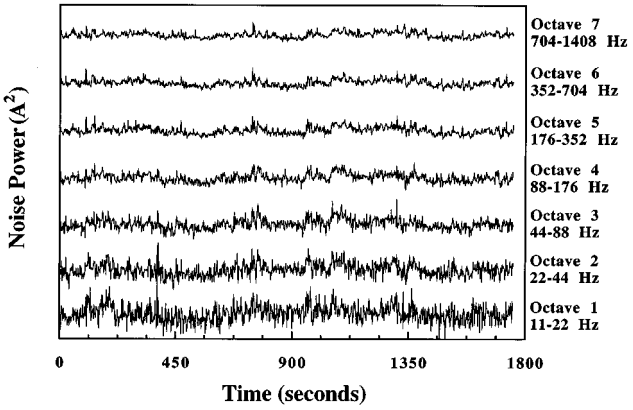

FIG. 2. Noise power octave time records plotted on a logarithmic scale at 435 K, 0.3 μA, and $N=4096$ spectra for the undoped a-Si:H sample. The curves have been offset for clarity. Also, for ease of plotting and to enhance visual correlations, each data point is the result of averaging four neighboring points.

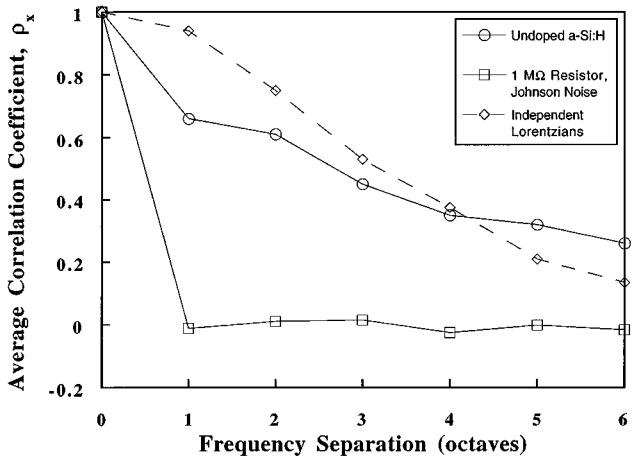

FIG. 3. Average correlation coefficients for a 1-MΩ wire-wound resistor (squares), the predicted result for independently modulated Lorentzians (diamonds), and an example of data for the undoped a-Si:H sample (circles) at 435 K calculated from Fig. 2. The measurements for the resistor, a known Gaussian noise source, consist of $N=2048$ spectra and the uncertainties in the ρ_x are within the expectation for Gaussian noise.

quency bins into octaves. For example, for a 1.56-kHz bandwidth and a sampling rate of 2.38 Hz (the time to acquire a single noise power spectrum), octave 1 is formed from the sum of three bins between approximately 11 and 22 Hz, octave 2 is formed from the sum of six bins between 22 and 44 Hz, and so on. The result of acquiring successive spectra is a series of time records of the noise power per octave (Fig. 2) that describes the spectral wandering of the system and contains the statistical information of the noise.

The time record of the noise power fluctuations (Fig. 2) displays strong correlations of the noise power between differing frequency octaves. For example, at a given time a fluctuation in one direction occurs in octaves 1, 2, and 3, but not in the other octaves, in which case octaves 1, 2, and 3 are positively correlated. These correlations are quantified by calculating correlation coefficients, defined as the covariance between octave i and octave j normalized by the standard deviations of octaves i and j:

$$\rho_{i,j}=\frac{\Sigma_{n=1}^{N_s}(Q_{i,n}-\langle Q_i\rangle)(Q_{j,n}-\langle Q_j\rangle)/(N_s-1)}{\sigma_i\sigma_j}, \quad (1)$$

where $Q_{i,n}$ is the noise power in octave i for spectrum n, $\langle Q_i\rangle$ is the average noise power in octave i over all N_s spectra, σ_i is the standard deviation in octave i, the octave indices i and j run from 1 to 7, and the sum is over all N_s spectra (typically $N_s=1024$). The $\rho_{i,j}$ vary from -1 to $+1$, signifying variations from perfectly anticorrelated ($\rho_{i,j}=-1$) to perfectly correlated ($\rho_{i,j}=+1$) behavior. Note that $\rho_{i,i}=1$ always since an octave noise power is completely correlated with itself, while for Gaussian (that is, uncorrelated) noise, the $\rho_{i,j}$ are zero for $i\neq j$. Details of the $\rho_{i,j}$ matrices are described elsewhere.[5,23]

The correlation coefficients $\rho_{i,j}$ are summarized by average correlation coefficients ρ_x, where ρ_x is the average $\rho_{i,j}$ over fluctuator bands separated by x octaves ($x=|i-j|$) in frequency space. In other words, the ρ_x are the averages along each diagonal of the $\rho_{i,j}$ matrix. For Gaussian noise, $\rho_x=0$ for $x\neq 0$ as verified by data shown in Fig. 3 for a 1-MΩ wire-wound resistor, which is a known Gaussian ''thermal'' noise source with a frequency independent (''white'') power spectrum of magnitude $4k_BTR$ (also commonly referred to as Johnson or Nyquist noise), where R is the resistance and T is the temperature. If the $1/f$ noise is due to a distribution of Lorentzian fluctuators whose amplitudes are independently modulated, then the resulting average correlation coefficients are given by $r/\sinh(r)$, where $r=\ln(f_i/f_j)$ and f_i and f_j are the center frequencies of octaves i and j.[4,28] These non-Gaussian, independent Lorentzian correlations arise due to overlap between the individual Lorentzians and fall off with octave separation as shown in Fig. 3. In Fig. 3 an example of the average noise correlation coefficients is shown for the n-type a-Si:H sample; similar results are found for the p-type and undoped samples. We find that the average correlation coefficients for a-Si:H are typically less correlated than the independent Lorentzian correlations at small octave separations and are more strongly correlated than the independent Lorentzian correlations at large octave separations.[29] Although not presented in this paper, another useful coefficient to calculate is the normalized variance for a given octave. These are related to the second spectrum described below.[23]

As stated in the Introduction, the electronic properties of a-Si:H exhibit glasslike behavior. The glassy behavior of the electronic conductivity is observed as a kink (which defines the equilibration temperature T_E) in an Arrhenius conductivity plot, giving two distinct regions with different activation energies and preexponential factors.[17] T_E separates the ''frozen-in'' low-temperature conductivity, whose magnitude depends on the cooling rate following a high-temperature annealing, from the ''equilibrium'' high-temperature conductivity, whose value is independent of thermal history. The undoped film exhibits a T_E of 445 K, while the n-type film has a T_E of about 390 K and for the p-type film $T_E\sim 350-360$ K. Because of this glassy nature, a consistent measurement procedure, which we term a ''thermal cycle,'' has been established. Before measuring the noise, the sample is first annealed in the dark at a high tem-

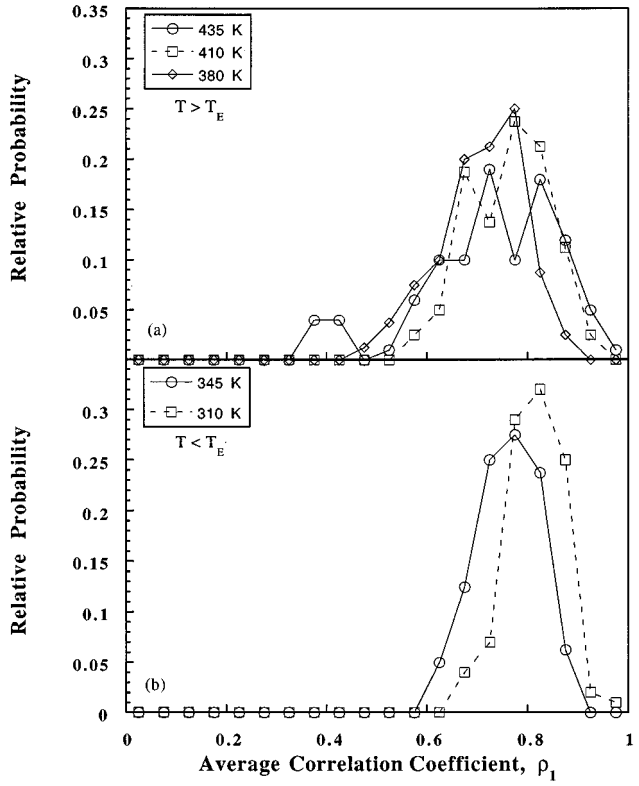

FIG. 4. Distributions for average correlation coefficient for a frequency separation of one octave ρ_1 from five thermal cycles as described in the text for the n-type a-Si:H film at temperatures of (a) 435, 410, and 380 K and (b) 345 and 310 K.

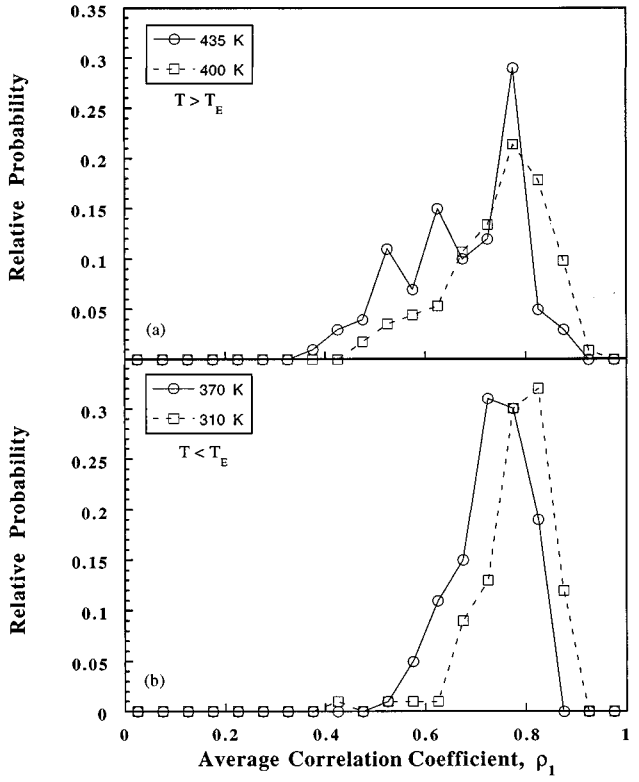

FIG. 5. Distributions for average correlation coefficient ρ_1 as described in the text for the p-type a-Si:H film at temperatures of (a) 435 and 400 K and (b) 370 and 310 K.

perature above T_E (495 K for undoped a-Si:H and 445 K for n-type and p-type a-Si:H) for 15 or 30 min (undoped or doped films, respectively) before cooling (cooling rate $\sim 10\,^{\circ}$C/min) to a set quenching temperature below T_E. The temperature is then slowly brought to the desired measurement temperature. As mentioned above, the large resistance of the undoped film necessitates higher temperatures to reliably carry out noise measurements at current levels comparable for the doped samples. The applied voltage is adjusted to maintain a constant current and after a fixed delay time of 1 h the data are collected. The thermal cycle data is composed of 20 runs, each consisting of 1024 noise power spectra; approximately 7 min is required to collect data for a single run.

Due to the time-dependent variations of the noise power between runs, it is useful to examine distributions of the average correlation coefficients. Results for ρ_1 from the thermal cycles are shown in Figs. 4 and 5 for the n-type and p-type films, respectively. Similar results are found for the other ρ_x. Each histogram shown here is comprised of data accumulated from four or five thermal cycles yielding 80–100 correlation coefficient values.

In Fig. 4, ρ_1 is presented for the n-type a-Si:H at 310, 345, 380, 410, and 435 K, and a current of 2 μA. While there is overlap in the distributions, a general trend is observed: At low temperatures the distribution is sharply peaked and has a relatively small width or variance. As the temperature is increased, the run to run variations in ρ_x increase and the distributions become broader. Further, for the n-type film at temperatures above T_E the ensemble average $\langle \rho_1 \rangle$ value decreases and the width of the distribution increases with temperature. Similar results are found for the p-type film at 0.3 μA, as shown in Fig. 5 for measurements performed at 310, 370, 400, and 435 K. For the undoped a-Si:H sample at 0.3 μA, numerous thermal cycles were performed at 435, 440, 450, 460, 470, and 485 K yielding similar results to the n-type sample, but with more scatter in the data.[23] We note that the noise statistics are independent of current or the macroscopic electric field.

C. Second spectra

Visual inspection of Fig. 2 reveals low-frequency modulations of the noise power that are characterized by calculating the Fourier transform of the individual noise power octave time records, yielding the power spectral density of the $1/f$ noise. This power spectrum is termed the second spectrum S_2 and describes the fluctuations of the octave noise power.[4,6,8] As the PSD of the current fluctuations S_1 is given by the two-point current correlation function $\langle I(t)I(t+t')\rangle$ from the Wiener-Khintchine theorem,[21] the PSD of the noise power fluctuations is given by the Fourier transform of the two-point correlation function $\langle Q_i(t)Q_i(t+t')\rangle$, where Q_i is the integrated noise power over an octave band i, as explained in Sec. III B. The correlation function in $Q_i(t)$ is equivalent to a four-point correlation function in the current given by Beck and Spruit[30] as $\langle X_k X^*_{k-p} X^*_m X_{m-p}\rangle$ for frequency f_p, where X_k is the Fourier coefficient of the current $I(t)$.[4,8,30,31] While an analysis of the variance of fluctuations has been considered by various investigators,[32] Beck and Spruit were the first to use the notation S_2, while Weissman

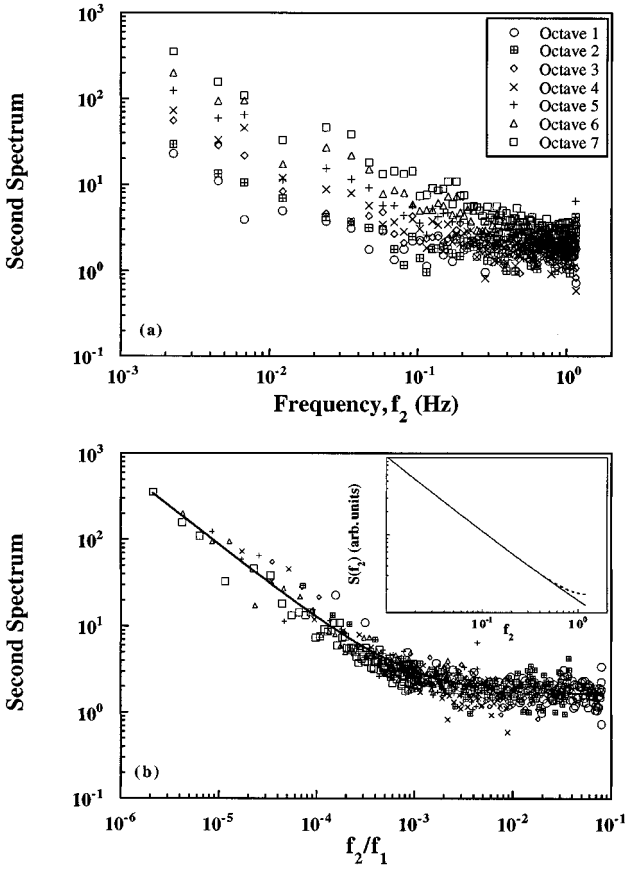

FIG. 6. (a) Normalized second spectra plotted against frequency f_2 for the undoped a-Si:H sample at 435 K as calculated from the data of Fig. 2 and as described in the text. The standard deviation of the mean for each second spectral density is approximately 10% of the S_2 magnitude. (b) Corresponding scaled second spectrum plotted against the ratio of frequencies f_2/f_1 with an unweighted least-squares fit. The frequency axis of each curve of (a) has been scaled by the appropriate octave center frequency f_1. The fitting results are $S_2(0)=1.6$, $\alpha_2=0.003$, and $\gamma_2=0.9$ compared to $\gamma_1=1.04$. Inset: effect of aliasing on a signal with a $1/f_2$ spectral density as described in the text. The solid line is the unaliased spectrum, while the dashed line is the aliased spectrum.

and co-workers later termed such an analysis ''second spectral analysis'' and devised the method of obtaining the second spectrum used in this work.

The second spectrum of each of the noise power octave time records of Fig. 2 is shown in Fig. 6(a) for the undoped a-Si:H sample. This second spectrum represents data taken during a thermal cycle and was constructed from a time record of 4096 data points sampled at approximately 2.3 Hz. Nearest-neighbor averaging was performed for displaying the S_2. Each S_2 in Fig. 6 is normalized by the expected variance for a Gaussian noise source, so that S_2 should have a magnitude of unity for Gaussian fluctuations, which would have a frequency-independent (white) second spectrum.[23,33] The normalized S_2 is dimensionless.

The S_2 of Fig. 6 clearly demonstrate the strong non-Gaussian nature of the $1/f$ noise in a-Si:H. The normalized S_2 have a general power-law form and magnitudes larger than unity. For all the a-Si:H films studied here, the magnitude and power-law exponent of the normalized S_2 are greatest for octave 7 and systematically decrease down to octave 1. The changes in the magnitude are a consequence of the Gaussian normalization; the unnormalized S_2 would give the largest magnitude to octave 1 since its fluctuations are largest (this octave consists of the fewest FFT points), as readily observed in Fig. 2. Further, the flattening of the second spectra with lower-frequency octaves is consistent with visual inspection of Fig. 2.

The second spectra in a-Si:H exhibit a scaling behavior, which we now describe. Each octave band Q_i may be described by its center frequency f_1, which is the geometric average of the end points of the octave band. For $1/f$ noise, the center frequency divides an octave into two regions of equal total noise power. By scaling each octave S_2 by its individual center frequency, the spectra collapse onto a single curve described by[1]

$$S_2(f_2,f_1)=S_2(0)+\alpha_2\left(\frac{f_2}{f_1}\right)^{-\gamma_2}, \tag{2}$$

as shown in Fig. 6(b). This indicates that slow fluctuators (at f_2) and fast fluctuators (at f_1) are governed by the same dynamics, which depends only on the ratio f_2/f_1. In other words, for a given magnitude of S_2 for different octave time records, the ratio of the center frequencies of the octaves is equal to the ratio of the f_2's for these octaves: $S_{2,i}(f_{2,i}/f_{1,i})=S_{2,j}(f_{2,j}/f_{1,j})$ and $f_1(\text{octave } i)/f_1(\text{octave } j)=f_2(\text{octave } i)/f_2(\text{octave } j)$. For the data shown in Fig. 6(b), $S_2(0)=1.6$, $\alpha_2=0.003$, and $\gamma_2=0.9$, as obtained from a least-squares fit. The S_2 for all n-type, p-type, and undoped a-Si:H films studied here are similar, although the undoped a-Si:H second spectra are typically two to three times smaller in magnitude than the doped a-Si:H second spectra. Further, no consistent temperature dependence of the S_2 is observed for these samples. We typically find $S_2(0)$ to vary from 1.5 to 6, while α_2 varies widely from 0.001 to 0.06. The corner frequency is that frequency of the second spectra at which the power-law region changes over to the frequency-independent portion of the second spectrum. From the scaled second spectra, the corner frequency varies from $f_2/f_1=10^{-3}$ to 10^{-2}. An important point discussed in Sec. IV is that for the vast majority of the S_2, the slope of the second spectrum is less than or equal to the first spectral slope, i.e., $\gamma_2\leqslant\gamma_1$.

Aliasing in the S_2 due to limitations of the sampling rate coupled with difficulty in knowing the exact frequency bandwidth of the octave noise power time records is negligible for the data of this study. We have investigated this issue using two standard techniques discussed in numerous references regarding signal processing, such as Ref. 34. For the first method we treat the noise power octave time records (see Fig. 2) as if they represent a discretized sequence derived from an analog signal that is sampled at a given rate. For our experimental sampling rate the effect of aliasing in the second spectrum is shown in the inset of Fig. 6(b) for a $1/f_2$ signal. The flattening of the spectrum at high frequencies is minor. This is also evident in the S_2 for octave 7 (see Figs. 6 and 9), which has the smallest unnormalized S_2 magnitude and is the most susceptible to aliasing effects. The

S_2 for octave 7 has a nearly uniform power-law form. Nevertheless, given the scatter in the data, we cannot rule out minor aliasing effects.

A second method of investigating the effects of aliasing in the second spectrum is downsampling or decimation of time record in which the effective sampling rate can be reduced by a factor M simply by considering every Mth point of the noise power octave time records of Fig. 2 in the calculations for the second spectra. As the time records are increasingly downsampled, one should be able to observe qualitatively systematic increases in the magnitude and a flattening of the high-frequency portions of the second spectra. For the noise in a-Si:H studied here, downsampling by a factor of $M=2$ (which reduces the octave time records in Fig. 2 from 4096 data points to 2048 data points) does not result in any marked changes in the second spectra, again indicating that any aliasing of the second spectra is small and may be neglected.

IV. DISCUSSION

Conduction in amorphous silicon has been suggested to occur, at least in part, through filamentary conduction paths analogous to the infinite cluster in a percolation network,[35,36] where fluctuators near or within these filaments modulate the conduction pathways, giving rise to the $1/f$ noise dynamics.[2,37] In Sec. IV A we discuss the structural and dynamic nature of the current filaments in a-Si:H. Many different models of spontaneous fluctuations that have a $1/f$ noise power spectral density in metals, semiconductors, and glasses describe the noise power spectrum or two-point autocorrelation function[7] for these materials. Hence the standard noise power spectrum alone is insufficient for distinguishing various theories. However, the statistical techniques utilized in this work can be used to discriminate between models of $1/f$ noise. Using the noise statistics, in Sec. IV B the $1/f$ noise dynamics are interpreted in terms of a serial (hierarchical) kinetics model.

A. Filamentary conduction in a-Si:H

The origin of the current filaments in this heterogeneous material may be both structural and electronic in nature and has been discussed in detail previously.[2] The electronic inhomogeneities in doped a-Si-H may arise due to charged dopants and oppositely charged dangling bonds[38] and in undoped a-Si:H due to charged dangling bonds.[39] For example, for the n-type doping levels used in this work, potential fluctuations due to charged impurities may have a period of thousands of angstroms and an amplitude of approximately 0.2 eV.[40,41] Structural inhomogeneities arise due to both the intrinsic disorder of the Si-Si network and the hydrogen microstructure. Hydrogen comprises approximately 10–20 at. % of the a-Si-H with roughly 3–4 at. % in a dilute phase of isolated Si-H bonds and the remainder in a clustered phase of at least six hydrogen atoms per cluster.[42,43] The results of Sec. III indicate that the dopants in a-Si:H have a small but noticeable effect on the $1/f$ PSD, as shown in Fig. 1, but do not appear to have any strong influence on the higher-order noise statistics. Consequently, the electronic states of the dopant do not appear to play a critical role in the non-Gaussian noise statistics.

The addition of dopant gases in the deposition plasma is known to effect the film microstructure and the deposition rate. This is especially true for p-type, boron-doped a-Si:H, which has a more heterogeneous microstructure[44,45] than n-type and undoped a-Si:H. Noise and electronic transport studies on a series of a-$Si_{1-x}C_x$:H films for which the carbon and hydrogen contents vary[46–48] have found that it is difficult to decouple the effects of microstructural and electronic changes in a-Si:H. Further investigation of this issue is currently in progress on a series of hot-wire chemical vapor deposition a-Si:H films that show non-Gaussian $1/f$ noise and for which the hydrogen content varies.[23,49]

It is plausible that hydrogen motion underlies the changes in the microchannel conductance. To account for the correlated or cooperative noise behavior, Fan and Kakalios have proposed that bonding rearrangements due to hydrogen motion within a given current filament may induce changes in the Si-Si strain fields, influencing the likelihood of other hydrogen atoms moving either on a neighboring current filament[37] or within the same filament, thereby giving rise to correlated conductance fluctuations. This could include hydrogen motion breaking a critical link (bond) in the filament, altering the conduction path, and affecting a region of the film that itself was contributing broadband noise spanning more than two octaves. Their experiment involved light soaking n-type-doped a-Si:H to generate light-induced defects, which could break weak filaments and increase the medium- or long-ranged disorder at the mobility edge. Consequently, the effect of changes in a filament on another region of the film would be reduced. Upon illumination and subsequent noise measurements in the dark, the $1/f$ noise correlation coefficients became weakly Gaussian; the second spectrum became flat (white), but its magnitude remained above unity. These light-induced changes in the conductivity and the $1/f$ noise statistics were reversible upon high-temperature annealing.

Recent dynamical percolation simulations of the conductivity of a-Si:H strongly implicate local hydrogen motion as responsible for the intermittent RTSN.[13] These simulations utilized experimentally determined a-Si:H parameters such as the Urbach slope (which characterizes the disorder of the Si-Si network) and local hydrogen hopping times determined from NMR spin-relaxation experiments.[18,19] We note that the explanation of the frequency correlations described above depends on the presence of filamentlike structures and does not rely on the system existing at the percolation threshold. Other experimental studies[50] and computer simulations[51] have found that hydrogen diffusion is sensitive to electronic changes and furthermore that a change in the charge state of a single defect can result in the rearrangement of hundreds of neighboring atoms. It is therefore possible (though unproven) that local hydrogen motion can induce sufficient alterations in the local electronic density of states to affect the conductance of inhomogeneous current filaments that arise from medium- and long-ranged disorder.

B. Hierarchical kinetics in a-Si:H

The observation of deviations of the correlation coefficients from the independently modulated Lorentzian fluctuator prediction (Fig. 3) indicates that the $1/f$ noise is not sim-

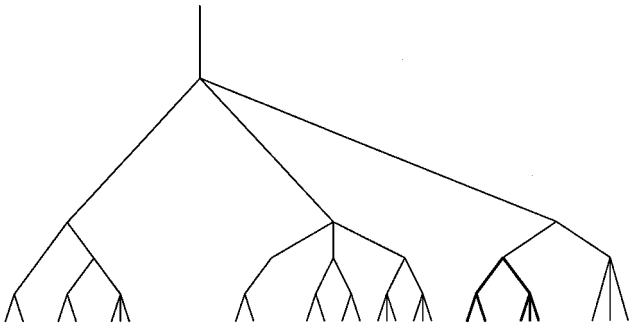

FIG. 7. Sketch of a portion of a hierarchical tree as described in the text. The darkened portion of the tree may represent regions accessible at lower temperatures, while larger regions (more states) can be sampled at higher temperatures.

ply due to a set of parallel, independently modulated Lorentzian fluctuators, but rather the noise sources interact through some form of serial kinetics.[1,4,7] Moreover, the nature of this serial interaction must account for the power-law frequency dependence of the second spectra [Fig. 6(a)] as well as its scaling behavior [Fig. 6(b)]. We now describe a model that accommodates much of the a-Si:H noise statistics data. We report evidence that both supports and challenges the model.

The serial behavior of the noise statistics may be described on a treelike structure such as a hierarchical or ultrametric space, as shown in Fig. 7.[52] The bottom level end points or leaves of the tree signify the various configurations or states of the system, for example, arrangements of hydrogen and Si atoms giving a particular defect structure and electronic conductance. The distance between vertices of the tree branches may represent barriers that the system must overcome in order to transform from one configuration to another. Typical descriptions of hierarchical trees assert that larger energies or longer times are required in order to surmount higher and higher vertices of the tree. Klafter and Shlesinger[53] have shown that hierarchical dynamics are equivalent to a multiple trapping dispersive diffusion model for stretched exponential behavior, as in a-Si:H. Bachas and Huberman[11] have demonstrated that for hierarchical trees with an effectively long and thin shape, only $1/f$ spectra may be produced. Further, disordered systems in general may be describable on such spaces. We now consider the noise dynamics on a hierarchical space along with the noise in a-Si:H.

Weissman has noted two key signatures of noise statistics that are general to such hierarchical dynamics models.[4] First, over time for a given sample, the system will sample different states or branches of the tree. For a structure with nonidentical branches there will be marked deviations of the noise power from the ensemble-average noise power. Consequently, the non-Gaussian noise statistics will vary with time (spectral wandering) and in a manner that can give information about the structure of the tree. Second, the slope of the second spectrum γ_2 should be less than the slope of the first spectrum γ_1, that is, $\gamma_2 < \gamma_1$. This is a consequence of the fact that the autocorrelation (or memory) function for the current $I(t)$ has a longer tail than the memory function for the noise power $S(f)$ or $Q_i(f_2, f)$. In other words, the probability of the system returning to its starting branch is greater at longer times for $I(t)$ than for the noise power since $I(t)$ is not frequency dependent and therefore will have more nearby states or branches that have similar $I(t)$ than will the noise power. While both of these points necessarily characterize a hierarchical space, alone they are not sufficient conditions to prove that such dynamics operate in the space.

These two key characteristics of hierarchical kinetics are observed in all a-Si:H samples studied in this work, confirming and expanding upon preliminary findings previously reported on n-type a-Si:H.[54] Not only are the noise statistics non-Gaussian as reflected in the correlation coefficients and the power-law second spectrum, but they also vary in time as evidenced by the distributions of noise correlation coefficients shown in Figs. 4 and 5 and by the variability of the noise power spectral density described in Sec. III A for the data shown in Fig. 1. We indeed find that $\gamma_2 \leqslant \gamma_1$ for over approximately 75% of the runs at any temperature for the n-type, p-type, and undoped a-Si:H films. Again, the spectral slopes γ_2 and γ_1 do not display a discernible temperature dependence.[23]

The scaling of the second spectrum (Fig. 6) is also consistent with a generic hierarchical tree even if the hierarchy is not completely self-similar, as argued by Weissman.[4] Qualitatively, the space or subsets of the space will have some degree of scale invariance and will have a fractal nature. On such a space, it is reasonable to expect that the dynamics of slow and fast fluctuators are equivalent given an appropriate scaling, of which f_2/f_1 is the most natural. This scaling of S_2 has been observed in the spin-glass CuMn,[55] while the scaling does not hold for various amorphous conductors at low temperatures.[56] Whether or not the scaling of the second spectrum is unique to glassy materials such as CuMn or a-Si:H is not yet clear. Further theoretical development and experimental studies on other systems must be performed to investigate this issue.

The deviations of the non-Gaussian correlation coefficients from the independent Lorentzian fluctuator prediction also may be consistent with dynamics on a hierarchical tree. For example, over long periods of time, the system may ascend higher and higher vertices and enter new states involving a different set of dominant fluctuators. Consequently, the correlations may be greater than independent Lorentzian correlations because wideband sets of frequency fluctuators will be influenced together. Over short periods of time, only small portions of the tree will be sampled; that is, only few, low vertices will be ascended and broadband correlations will not be as strong. The correlations will not be larger than Lorentzian correlations and may even be smaller, possibly due to the influence of negative correlations.[4] Thus there may be a crossover behavior of the average correlation coefficient from values lower than that predicted by independently modulated Lorentzians to values greater than that predicted by independently modulated Lorentzians.

To test this argument, averaging out fast fluctuations of the octave time records and recalculating the correlation coefficients should yield correlations that grow with averaging time since longer times are being probed, corresponding to the system traversing higher vertices of the hierarchical tree. Such behavior is found for our data on a-Si:H, as shown in Fig. 8, and has also been seen by Parman, Israeloff, and Kakalios.[1] As the faster fluctuations of the noise power are

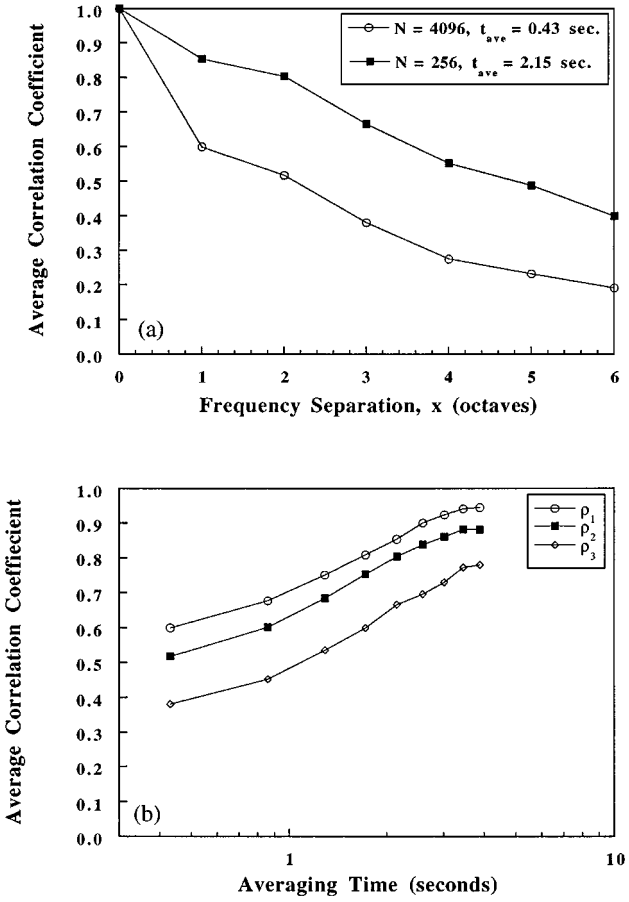

FIG. 8. (a) Average correlation coefficients as a function of averaging time for the data shown in Fig. 2. The quasilogarithmic increase in the ρ_x with averaging time is shown in (b) for ρ_1, ρ_2, and ρ_3.

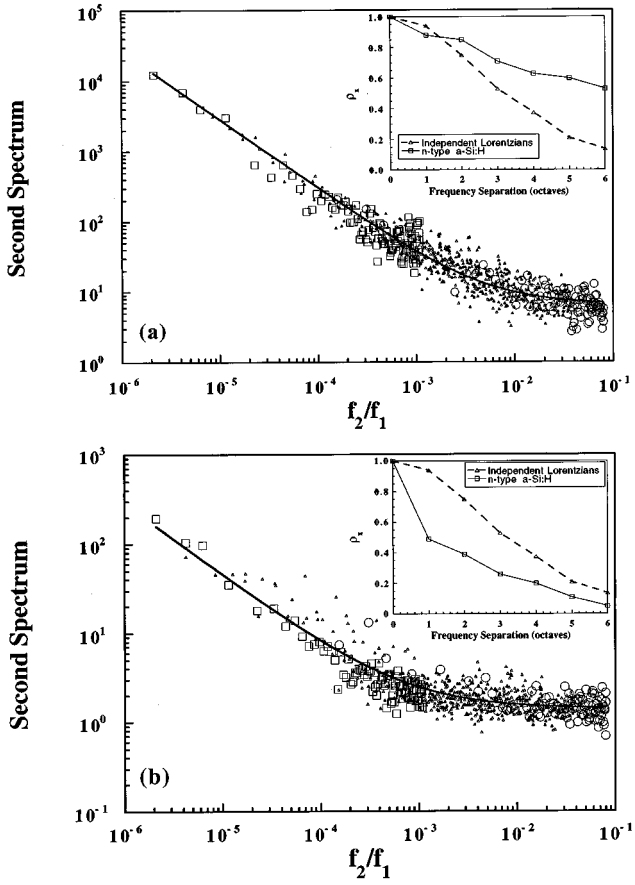

FIG. 9. Scaled and normalized second spectrum during two runs of $N=4096$ spectra for the n-type sample at 435 K as described in the text. For visual clarity, octave 7 data are represented by squares, octave 1 data are represented by circles, and octaves 2–6 are represented by small triangles. The fit parameters for the S_2 are (a) $S_2(0)=6.5$, $\alpha_2=0.036$, and $\gamma_2=0.98$ and (b) $S_2(0)=1.4$, $\alpha_2=0.004$, and $\gamma_2=0.81$, as demonstrated by the solid lines. Insets: average correlation coefficients for each run plotted against octave separation along with the theoretically expected results for independently modulated Lorentzian fluctuators.

removed, the average correlation coefficients increase. This increase follows a quasilogarithmic dependence on time, as shown in Fig. 8(b). Logarithmic time dependences are characteristic of certain hierarchical spaces. It is not yet clear how and if the dynamics of the average correlation coefficients map onto this description. We note that in some of the cases for which $\gamma_2 > \gamma_1$ quasilogarithmic time dependences similar to that of Fig. 8(b) are also found, suggesting that either the system is not well described by an hierarchical space during these particular runs or that quasilogarithmic time dependences may not be unique to a hierarchical space.

The deviations of the correlation coefficients from the independent Lorentzian correlations are also consistent with the second spectra. Correlations larger than the independent Lorentzian correlations correspond to the power-law portion of the second spectrum because this portion represents the slower or longer-time dynamics of the system, which, as described above, are more correlated. The smaller correlation coefficients correspond to the white part of the second spectrum[4] since the frequency-independent portion occurs at higher frequencies f_2 and describes the faster or shorter-time dynamics that occur as the system is sampling only a small region of the hierarchical space. Thus one would expect an S_2 of comparatively larger magnitude for a system that is relatively highly correlated and an S_2 of smaller magnitude for a system that is relatively weakly correlated, compared to independently modulated Lorentzian correlations. This is demonstrated in Fig. 9 for two different runs during two different thermal cycles for the n-type a-Si:H film at 435 K. The frequency correlation coefficients ρ_x are larger for the run shown in Fig. 9(a) than for the run shown in Fig. 9(b). The data in Fig. 9(a) therefore may represent a time when the system is sampling many states and traversing higher vertices of the tree than for the data in Fig. 9(b). In Fig. 9(b) the correlation coefficients are smaller, indicating that the system was not able to traverse high vertices and was confined to a small region of the tree and, consequently, would have a smaller magnitude second spectrum than for the data of Fig. 9(a). Further evidence that the system is more correlated as it samples more states of the tree is seen from the slopes and cutoff or corner frequencies of the second spectra of Fig. 9. The difference in the slopes of the two second spectra indicate that the memory function of the fluctuating system has a longer time tail for the data of Fig. 9(a) ($\gamma_2=0.98$) than that of Fig. 9(b) ($\gamma_2=0.81$). Also, the scaled corner frequency for the data of Fig. 9(a) ($f_2/f_1 \sim 5\times10^{-3}$) is higher than for the data of Fig. 9(b) ($f_2/f_1 \sim 10^{-3}$). The corner frequency

may provide information regarding the branching structure of the hierarchical tree, although such an interpretation would require further theoretical development.

Two additional points of discussion are warranted regarding the data of Fig. 9. First, generally the second spectral magnitudes fall in between those of Figs. 9(a) and 9(b) and most correlation coefficients ρ_x take on values that cross over the independent Lorentzian prediction between approximately $x=3$ and 4 octave separations, as shown in Fig. 3. This finding may also provide information regarding the structure of the tree and suggests that relative to the Lorentzian correlations, nearest- and next-nearest-neighbor fluctuators are less correlated than fluctuators further apart in frequency. Second, while the data presented represent specific states of the *a*-Si:H system at a high temperature of 435 K, all of the *a*-Si:H data obtained in this study indicate that the second spectra and the magnitude of the correlation coefficients are not temperature dependent. There is a finite probability for the system to overcome barriers and sample states on the hierarchical tree at any temperature probed in this study, and similar data have been found at 310 K. Thus it is possible for data such as those shown in Fig. 9 to be found at other temperatures. This lack of a temperature dependence of the *a*-Si:H second spectra, which is predicted in general for hierarchical spaces, is a major problem with the above analysis. A temperature dependence of the stretched exponential relaxation of the conductivity is clearly observed in *a*-Si:H, in agreement with the corresponding hierarchical kinetics model of Klafter and Shlesinger.[53] A temperature dependence of the second spectrum is also observed in the spin-glass CuMn.[55] In that system, second spectra of *comparable magnitudes* were found at two different temperatures (23 and 11 K) with a smaller γ_2 at the higher temperature. This indicates that the spin glass explores comparable portions of the hierarchical tree independently of temperature, but that the spectral memory function is weaker at the higher temperature.

Further, in *a*-Si:H a distinct temperature dependence of the correlation coefficients is absent. At best, as shown in Figs. 4 and 5, a weak trend in the width of the correlation coefficients distributions as a function of temperature is observed. At lower temperatures the distributions are narrower and more sharply peaked, while at higher temperatures the distributions are broader. A possible but speculative explanation of these data is that from run to run the system may only be able to sample relatively few states at lower temperatures compared to higher temperatures.

While none of the data presented offer conclusive evidence of hydrogen's role in the $1/f$ and $1/f$ noise statistics, these experiments do not rule out the influence of hydrogen in the noise, especially local hydrogen motion that is weakly temperature dependent.[18,19] Overall, while disordered systems may generally be describable on hierarchical spaces, the actual construction of the space for *a*-Si:H is not clear and theoretical models specific to *a*-Si:H must be developed in order to clarify this issue further. Nevertheless, we have demonstrated several characteristics of the noise in *a*-Si:H that are consistent with dynamics on a hierarchical space.

V. SUMMARY

In summary, low-frequency conductance fluctuations of *a*-Si:H films from two different deposition reactors have been studied. The $1/f$ noise magnitude in *n*-type, *p*-type, and undoped hydrogenated *a*-Si:H depends weakly on the dopant type and temperature. The dopant does not play a critical role in the non-Gaussian $1/f$ noise statistics. Higher-order statistical tests involving the second spectrum and frequency correlations have several key characteristics indicating that the noise is governed by serial or hierarchical kinetics. First, the $1/f$ noise itself shows spectral wandering; i.e., the $1/f$ noise is time dependent. Second, strong deviations of the non-Gaussian correlation coefficients from the independently modulated Lorentzian correlations indicate that the fluctuators are modulated in series rather than through parallel, independent modulations. Third, these series modulations lead to $1/f$ second spectra that exhibit scaling behavior. Fourth, the system is more correlated as longer time dynamics are probed. Fifth, the distributions of the correlation coefficients have a weak temperature dependence that may be qualitatively consistent with dynamics on a hierarchical space. The lack of a temperature dependence of the second spectrum, the few cases in which $\gamma_2 > \gamma_1$, and a weak temperature dependence of the correlation coefficients remain unexplained by the given hierarchical kinetics model.

Any model of the low-frequency conductance fluctuations in *a*-Si:H must predict or incorporate these characteristics described above. To date and to our knowledge, the hierarchical model best describes the $1/f$ noise in *a*-Si:H. Finally, the noise data are consistent with a model of electronic conduction via dynamical filamentary conduction pathways that may be modulated by local hydrogen motion.

ACKNOWLEDGMENTS

We thank C. E. Parman, N. E. Israeloff, M. B. Weissman, A. H. Tewfik, and G. Venkatesan for helpful discussions. We thank C. C. Tsai and R. A. Street of Xerox PARC for providing the doped *a*-Si:H films. This work was funded in part by NSF Grants Nos. DMR-9057722 and DMR-9424277. G.M.K. was supported in part by the U.S. Department of Education.

*Present address: Seagate Technology, Minneapolis, MN 55435.

[1] C. E. Parman, N. E. Israeloff, and J. Kakalios, Phys. Rev. Lett. **69**, 1097 (1992).

[2] C. E. Parman, N. E. Israeloff, and J. Kakalios, Phys. Rev. B **47**, 12 578 (1993).

[3] G. M. Khera and J. Kakalios, in *Amorphous Silicon Technology—1994*, edited by E. A. Schiff, M. Hack, A. Madan, M. J. Powell, and A. Matsuda, MRS Symposia Proceedings No. 336 (Material Research Society, Pittsburgh, 1994), p. 395.

[4] M. B. Weissman, Rev. Mod. Phys. **65**, 829 (1993).

[5] P. J. Restle, M. B. Weissman, and R. D. Black, J. Appl. Phys. **54**, 5844 (1983).

[6] P. J. Restle, R. J. Hamilton, M. B. Weissman, and M. S. Love, Phys. Rev. B **31**, 2254 (1985).

[7] M. B. Weissman, Rev. Mod. Phys. **60**, 537 (1988).
[8] M. B. Weissman, N. E. Israeloff, and G. B. Alers, J. Magn. Magn. Mater. **114**, 87 (1992).
[9] R. G. Palmer, D. L. Stein, E. Abrahams, and P. W. Anderson, Phys. Rev. Lett. **53**, 958 (1984).
[10] A. T. Ogielski and D. L. Stein, Phys. Rev. Lett. **55**, 1634 (1985).
[11] C. P. Bachas and B. A. Huberman, Phys. Rev. Lett. **57**, 1965 (1986).
[12] C. E. Parman, N. E. Israeloff, and J. Kakalios, Phys. Rev. B **44**, 8391 (1991).
[13] L. M. Lust and J. Kakalios, Phys. Rev. Lett. **75**, 2192 (1995).
[14] L. M. Lust and J. Kakalios (unpublished).
[15] C. E. Parman and J. Kakalios, Phys. Rev. Lett. **67**, 2529 (1991).
[16] J. Kakalios, R. A. Street, and W. B. Jackson, Phys. Rev. Lett. **59**, 1037 (1987).
[17] R. A. Street, J. Kakalios, C. C. Tsai, and T. M. Hayes, Phys. Rev. B **35**, 1316 (1987).
[18] P. Hari, P. C. Taylor, and R. A. Street, in *Amorphous Silicon Technology—1995*, edited by M. Hack, E. A. Schiff, A. Madan, M. Powell, and A. Matsuda, MRS Symposia Proceedings No. 377 (Material Research Society, Pittsburgh, 1995), p. 185.
[19] P. Hari, P. C. Taylor, and R. A. Street, in *Amorphous Silicon Technology—1994* (Ref. 3), p. 329.
[20] M. B. Weissman (private communication).
[21] J. S. Bendat and A. G. Piersol, *Random Data: Analysis and Measurement Procedures*, 2nd ed. (Wiley, New York, 1986).
[22] M. Nelkin and A.-M. S. Tremblay, J. Stat. Phys. **25**, 253 (1981).
[23] G. M. Khera, Ph.D. thesis, University of Minnesota, 1996.
[24] D. A. Bell, *Electrical Noise: Fundamentals and Physical Mechanism* (Van Nostrand, London, 1960), Chap. 10.
[25] F. N. Hooge, T. G. M. Kleinpenning, and L. K. J. Vandamme, Rep. Prog. Phys. **44**, 479 (1981).
[26] G. M. Khera, H. M. C. Dyalsingh, and J. Kakalios (unpublished).
[27] G. M. Khera, H. M. C. Dyalsingh, and J. Kakalios, Bull. Am. Phys. Soc. **41**, 117 (1996).
[28] P. J. Restle, M. B. Weissman, G. A. Garfunkel, P. Pearah, and H. Morkoc, Phys. Rev. B **34**, 4419 (1986).
[29] We have found nearly Gaussian $1/f$ noise statistics on an n-type a-Si:H sample fabricated at The University of Chicago, as reported in Ref. 23. K. Abkemeier (unpublished) and R. Johanson *et al.* (unpublished) have found similar results on n-type doped samples of different doping levels from our sample but fabricated in the same deposition reactor. We further note that we have measured non-Gaussian $1/f$ noise from a variety of a-Si:H samples produced in four different deposition systems (Refs. 23 and 46–49).
[30] H. G. E. Beck and W. P. Spruit, J. Appl. Phys. **49**, 3384 (1978).
[31] G. T. Seidler and S. A. Solin, Phys. Rev. B **53**, 9753 (1996).
[32] See, for example, B. Mandelbrot, IEEE Trans. Inf. Theory **IT-13**, 289 (1967); J. J. Brophy, J. Appl. Phys. **41**, 2913 (1970); F. N. Hooge and A. M. H. Hoppenbrouwers, Physica (Utrecht) **42**, 331 (1969); U. J. Strasilla and M. J. O. Strutt, J. Appl. Phys. **45**, 1423 (1974).
[33] As a point of clarification in the ''second-spectrum literature,'' we note that at least three different normalizations are used for quantities simply referred to as second spectra. Weissman and co-workers have employed two different normalizations yielding dimensionless second spectra (Refs. 4 and 8). Seidler and Solen's second spectrum (Ref. 31) is similar to that of Beck and Spruit (Ref. 30), but gives the second spectrum in units of Hz^{-1}.
[34] John G. Proakis and Dimitris G. Manolakis, *Digital Signal Processing: Principles, Algorithms, and Applications*, 2nd ed. (Macmillan, New York, 1992).
[35] R. Zallen and H. Scher, Phys. Rev. B **4**, 4471 (1971).
[36] M. H. Brodsky, Solid State Commun. **36**, 55 (1980).
[37] J. Fan and J. Kakalios, Philos. Mag. B **69**, 595 (1994).
[38] R. A. Street, Phys. Rev. Lett. **49**, 1187 (1982).
[39] G. H. Schumm and G. H. Bauer, Phys. Rev. B **39**, 5311 (1989); Philos. Mag. B **64**, 515 (1991).
[40] H. Overhof and W. Beyer, Philos. Mag. B **43**, 433 (1981); H. Overhof, in *Amorphous Silicon Technology—1992*, edited by M. J. Thompson, Y. Hamakawa, P. G. LeComber, A. Madan, and E. A. Schiff, MRS Symposia Proceedings No. 258 (Material Research Society, Pittsburgh, 1992), p. 681.
[41] R. A. Street, J. Kakalios, and M. Hack, Phys. Rev. B **38**, 5603 (1988).
[42] J. A. Reimer, R. W. Vaughan, and J. C. Knights, Phys. Rev. Lett. **44**, 193 (1980).
[43] K. K. Gleason, M. A. Petrich, and J. A. Reimer, Phys. Rev. B **36**, 3259 (1987).
[44] E. A. Schiff, P. D. Persans, H. Fritzsche, and V. Akopyan, Appl. Phys. Lett. **38**, 92 (1981).
[45] J. B. Boyce and S. E. Ready, in *Amorphous Silicon and Related Materials*, edited by H. Fritzsche (World Scientific, Singapore, 1988), Vol. A, p. 29.
[46] H. M. C. Dyalsingh, G. M. Khera, J. Kakalios, C. C. Tsai, and R. A. Street, in *Amorphous Silicon Technology—1994* (Ref. 3), p. 631.
[47] H. M. C. Dyalsingh, G. M. Khera, and J. Kakalios, in *Amorphous Silicon Technology—1995* (Ref. 18), p. 577.
[48] G. M. Khera, H. M. C. Dyalsingh, D. Quicker, and J. Kakalios (unpublished).
[49] G. M. Khera, J. Kakalios, Q. Wang, and E. Iwaniczko, in *Amorphous Silicon Technology—1996*, edited by E. A. Schiff, M. Hack, A. Madan, M. J. Powell, and A. Matsuda, MRS Symposia Proceedings No. 420 (Material Research Society, Pittsburgh, 1996), p. 641; G. M. Khera and J. Kakalios (unpublished).
[50] P. V. Santos, N. M. Johnson, R. A. Street, M. Hack, R. Thompson, and C. C. Tsai, Phys. Rev. B **47**, 10 244 (1993).
[51] P. A. Fedders, Y. Fu, and D. A. Drabold, Phys. Rev. Lett. **68**, 1888 (1992); H. M. Branz and P. A. Fedders, in *Amorphous Silicon Technology—1994* (Ref. 3), p. 129.
[52] R. Rammal, G. Toulouse, and M. A. Virasoro, Rev. Mod. Phys. **58**, 765 (1986).
[53] J. Klafter and M. F. Shlesinger, Proc. Natl. Acad. Sci. USA **83**, 848 (1986).
[54] J. Kakalios, Braz. J. Phys. **23**, 137 (1993).
[55] N. E. Israeloff, Ph.D. thesis, University of Illinois at Urbana-Champaign, 1991.
[56] G. A. Garfunkel, G. B. Alers, and M. B. Weissman, Phys. Rev. B **41**, 4901 (1990).